

# Curcumin attenuates high glucose-induced inflammatory injury through the reactive oxygen species–phosphoinositide 3-kinase/protein kinase B–nuclear factor- $\kappa$ B signaling pathway in rat thoracic aorta endothelial cells

Zhen Zhang<sup>1\*</sup> , Keming Li<sup>2</sup>

<sup>1</sup>Department of Endocrinology, First People's Hospital, Shangqiu, Henan, and <sup>2</sup>Department of pharmacology, Research institute of traditional Chinese medicine, Jinan, Shandong, China

## Keywords

Curcumin, Inflammation, Rat thoracic aorta endothelial cells

## \*Correspondence

Zhen Zhang  
Tel.: +86-370-3255700  
Fax: +86-370-3255700  
E-mail address:  
ZhangzhenWINE@126.com

*J Diabetes Investig* 2018; 9: 731–740

doi: 10.1111/jdi.12767

## ABSTRACT

**Aims/Introduction:** Endothelial cell inflammatory injury is likely required for barrier dysfunction under hyperglycemic conditions. Curcumin (CUR) is well known for its anti-inflammatory effect. However, there have been few reports about the anti-inflammatory effect of CUR induced by high glucose in endothelial cells. The aim of the present study was to investigate the inflammatory effect of high glucose and the anti-inflammatory effect of CUR induced by high glucose in rat thoracic aorta endothelial cells (TAECS).

**Materials and Methods:** Well characterized TAECS were established and cell viability was assayed by the cell counting kit-8 method, messenger ribonucleic acid and protein expression were identified by real-time polymerase chain reaction, western blot or enzyme-linked immunosorbent assay, respectively. The production of reactive oxygen species was observed by a fluorescence microscope.

**Results:** High glucose (30 mmol/L) significantly decreased the cell viability of TAECS after being co-cultivated for 12 h and showed a time-dependent manner, and increased interleukin (IL)-1 $\beta$ , IL-6 and tumor necrosis factor- $\alpha$  secretion in TAECS. The injury effect of high glucose was involved in the reactive oxygen species–phosphoinositide 3-kinase (PI3K)/protein kinase B (AKT)–nuclear factor (NF)- $\kappa$ B signaling pathway. Anti-oxidant N-acetylcysteine, PI3K and NF- $\kappa$ B-specific pathway inhibitors can abolish the secretion of these inflammatory factors; pretreatment with anti-oxidant N-acetylcysteine significantly decreased PI3K expression, the level of phosphorylated AKT and nuclear NF- $\kappa$ B; pretreatment of LY294002 can significantly decrease the NF- $\kappa$ B level in nuclei. After treatment with CUR for 12 h, IL-1 $\beta$ , IL-6 and tumor necrosis factor- $\alpha$  secretion were markedly decreased, and PI3K expression, the phosphorylation of AKT and nuclear NF- $\kappa$ B level were also decreased.

**Conclusion:** Curcumin attenuates high glucose-induced inflammatory injury through the reactive oxygen species–PI3K/AKT–NF- $\kappa$ B signaling pathway in rat thoracic aorta endothelial cells.

## INTRODUCTION

Research has shown that the initiation and development of diabetes is a chronic inflammation progression<sup>1,2</sup>, and the

accumulation of glucose activates vascular inflammation through increasing the capability of endothelial adhesiveness to monocytes. The glycation end-products can exert an effect of inducing and amplifying the oxidant and inflammation in vascular endothelial cells<sup>3–5</sup>. The damaged endothelial cells induced

Received 14 September 2017; revised 8 October 2017; accepted 13 October 2017

by inflammation results in microvascular dysfunction. Impaired barrier function in the vascular wall, neutrophil influx into organs, impaired distribution of blood flow in microvascular beds, as well as microvascular thrombosis are the most common forms of microvascular dysfunction<sup>6,7</sup>. Endothelial dysfunction is an early step in many vascular diseases, and inflammation takes part in the pathological process of organ dysfunction mostly by motivating endothelial dysfunction<sup>8</sup>. Data from experimental research and clinics suggest that endothelial dysfunction is the initial step of activating coagulation, which is marked by a shift towards the pro-inflammatory state. For attenuating hyperglycemia-induced chronic vascular diseases is to find a strategy in dealing with redundant glucose-induced endothelial inflammatory injury.

Curcumin (CUR; chemical structure shown in Figure 5a) is a natural phytochemical of turmeric from the rhizomes of *Curcuma longa*, and has been reported to have a wide pharmacological effect, such as anti-inflammatory<sup>9–11</sup>, anti-oxidant<sup>12–14</sup>, and anti-carcinogenic properties<sup>15–17</sup>, and is widely used in treating arthritis, cancer, respiratory infections, and digestive and liver abnormalities. The anti-inflammatory effect of CUR is well documented, whereas the anti-inflammatory effect in the diseases of diabetes is not clear. Here, we explored the inflammatory effect of high glucose in rat thoracic aorta endothelial cells (TAECs) and the anti-inflammatory effect of CUR on high glucose-induced inflammation in TAECs, and furthermore, investigated whether high glucose elicited the endothelial inflammatory response or the anti-inflammatory effect of CUR through the phosphoinositide 3-kinase (PI3K)/protein kinase B (AKT) and nuclear factor (NF)- $\kappa$ B signaling pathway.

## METHODS

### Reagents

Curcumin was from the National Food and Drug Testing Institute, Beijing, China. Dulbecco's modified Eagle's medium (DMEM) 1,640 (the concentration of glucose is 5.6 mmol/L) was purchased from Hyclone (South Logan, UT, USA), and fetal bovine serum (FBS) was acquired from GIBCO BRL (Grand Island, NY, USA). Endothelial cells growth factor was bought from Roche Inc. (Basel, Switzerland). Trizol and the one-step reverse transcription polymerase chain reaction (PCR) kit were from Invitrogen (Carlsbad, CA). PI3K inhibitor LY294002, anti-oxidant N-acetylcysteine (NAC) and NF- $\kappa$ B inhibitor pyrrolidine dithiocarbamate (PDTC) were from Sigma-Aldrich (St. Louis, MO, USA). Rabbit NF- $\kappa$ B antibody and rabbit CD 31 antibody were provided by Abcam (Cambridge, MA, USA). Rabbit monoclonal  $\beta$ -actin antibody was ordered from Zhuangzhi Biotech (Xi'an, China). AKT and phospho-AKT antibodies, 2',7'-dichlorodihydrofluorescein (DCF) diacetate were obtained from Beyotime (Jiangsu, China). PI3K antibodies were from Cell Signaling Technology (Danvers, MA, USA). Relative second antibodies were provided by CW Biotech (Beijing, China). Enzyme-linked immunosorbent assay (ELISA) kits for detecting interleukin (IL)-1 $\beta$ , IL-6 and tumor

necrosis factor (TNF- $\alpha$ ) were from West Tang (Shanghai, China). All other materials, except where indicated, were of analytical grade.

### Primary rat TAECs

Rat TAECs were isolated from the thoracic aortae of male Sprague-Dawley rats based on previously described methods<sup>18</sup>, and were identified by immunofluorescence staining with CD 31 antibody (Figure S1). The cells were cultured in DMEM media supplemented with 20% FBS, 100 U/mL streptomycin, 100 U/mL penicillin, 95  $\mu$ g/mL heparin and 20  $\mu$ g/mL endothelial cells growth factor. The cells were maintained in a 5% humidified air CO<sub>2</sub> atmosphere at 37°C. Cells at passage 3–8 when at 80–90% confluence were used in the current study. All experimental procedures were strictly instructed by the international, national and institutional rulers, and approved by the Institutional Animal Care Committee of Henan University.

### Cell viability assay

The cell counting kit-8 method was used to detect the cell viability of TAECs after indicated treatment in 96-well plates. The experimental protocol was as follows: after indicated treatment, 10- $\mu$ L cell counting kit-8 solution was added to each well and followed by a further 4-h incubation at 37°C. The optical density was measured at 450 nm by a microplate reader (Molecular Devices, Sunnyvale, CA, USA). The mean optical density of six wells was used to calculate the cell viability percentage.

### Quantitative real-time PCR

The TAECs were cultured in six-well plates at the density of  $1 \times 10^5$  cells per well. After indicated treatment, the cells were washed twice with ice-cold phosphate-buffered saline, and the total messenger ribonucleic acid (mRNA) was extracted by Trizol reagent (Invitrogen, Carlsbad, CA, USA), according to the manufacturer's instructions. The concentration of RNA was determined by measuring the absorbance at 260 nm. The total RNA was then reverse transcribed to complementary deoxyribonucleic acid (cDNA) by high-capacity reverse transcriptase and 1  $\mu$ mol/L oligo (dT; Takara, Tokyo, Japan). The primer pair sequences were specific to rat IL-1 $\beta$  (F-5'-CCCAACTGGT ACATCAGCACCTCTC-3'; R-5'-CTATGTCCCACCATTG CTG-3'), IL-6 (F-5'-GATTGTATGAACAGCGATGATGC-3'; R-5'-AGAAACGGAACTCCAGAAGACC-3'), TNF- $\alpha$  (F-5'-AT GGGCTCCCCTCTCATCAGT-3'; R-5'-GCTTGGTGGTTTGC TACGAC-3') and glyceraldehyde-3-phosphate dehydrogenase (F-5'-TGGAGTCTACTGGCGTCTT-3'; R-5'-TGTCATATTTT CCGTGGTTCA-3'). cDNA was amplified and normalized to the level of glyceraldehyde-3-phosphate dehydrogenase. SYBR premix Ex taq (Takara Bio Inc., Shiga, Japan) was used in the current experiment, which was carried out in the Mx3000P quantitative PCR system (Stratagene, La Jolla, CA, USA). All samples were run in triplicate, and analyzed using the  $2^{-\Delta\Delta Ct}$  methods as previously described.

**Elisa**

TAECs were cultured in a 96-well plate and stimulated with high glucose for 12 h. Then, the supernatant was collected, and levels of IL-1 $\beta$ , IL-6 and TNF- $\alpha$  in the supernatant were assayed by ELISA kit specific for rat IL-1 $\beta$ , IL-6 and TNF- $\alpha$ .

**Measurement of intracellular reactive oxygen species**

The level of intracellular reactive oxygen species (ROS) was determined by oxidative conversion of cell-permeable DCF diacetate to fluorescent DCF. After indicated treatments, DCF diacetate (10  $\mu$ mol/L) in FBS-free DMEM was added to the six-well plate and the cells were incubated for 20 min at 37°C. Then, the six-well plates were washed three times with FBS-free DMEM, and DCF fluorescence was measured by using a fluorescent microscope (BX50-FLA; Olympus, Tokyo, Japan). Mean fluorescence intensity from six random fields was analyzed using Image J 1.41 software (National Institutes of Health, Bethesda, MD, USA), and mean fluorescence intensity was used to represent the amount of ROS.

**Immunofluorescence staining**

The TAECs were incubated with the primary rabbit anti-CD31 antibody overnight at 4°C and then with the secondary Alexa fluor 488 conjugated antibody for a further 3 h at room temperature. Subsequently, the cells were stained in 2-(4-amidino-phenyl)-6-indolecarbamidine dihydrochloride solution. Each step above was followed by washing three times. Finally, the

cells on coverslips were preserved in anti-fade mounting medium and CD31 expression was observed under fluorescent microscope (BX50-FLA; Olympus, Tokyo, Japan).

**Western blot**

After the indicated treatment, the cells were washed twice with ice-cold PBS (pH 7.4), and lysed with lysis buffer supplemented with protease inhibitor cocktail and phosphatase inhibitors (Roche, Basel, Switzerland) 100  $\mu$ L per well of a six-well plate. Concentration of the protein was measured by bicinchoninic acid assay protein assay kit (Bio-Rad, Hercules, CA, USA). An equal amount of the protein (30  $\mu$ g) was loaded, separated by 10% sodium dodecyl sulfate polyacrylamide gel electrophoresis, and blotted onto polyvinylidene fluoride membrane (0.45  $\mu$ m, GE Healthcare, Buckinghamshire, UK). The membranes were incubated with anti- $\beta$ -actin (1:2000), anti-AKT (1:1500), anti-phospho-AKT (1:800) or anti-PI3K (1:1000), anti-NF- $\kappa$ B (1:500) and anti-LaminB (1:1000) antibodies at 4°C overnight. After being washed three times, the membranes were incubated with the relevant horseradish peroxidase-conjugated second antibodies (1:3000) for 3 h, and then the immune complexes were enhanced by chemiluminescence.

**Statistical analysis**

The results are represented as mean  $\pm$  standard error of mean. Statistical analysis was carried out by Steer–Dwass or Mann–Whitney multiple comparison tests. This was carried out by

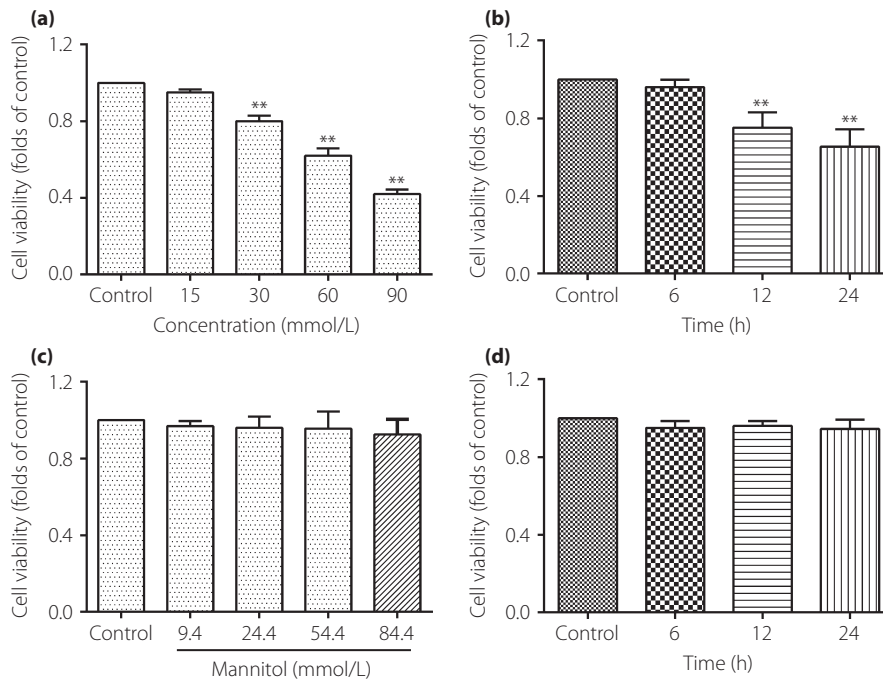


**Figure 1** | The effect of high glucose treatment on cell viability of thoracic aorta endothelial cells. (a) The cells were incubated with different concentrations of glucose for 12 h. (b) The cells were incubated with glucose concentrations of 30 mmol/L for 0, 6, 12 and 24 h. (c) The cells were incubated with different concentrations of mannitol for 12 h. (d) Cells were subjected to the mannitol concentrations of 24.4 mmol/L for 0, 6, 12 and 24 h. Results were from six independent experiments and expressed as mean  $\pm$  standard error of the mean. \*\**P* < 0.01 vs control.

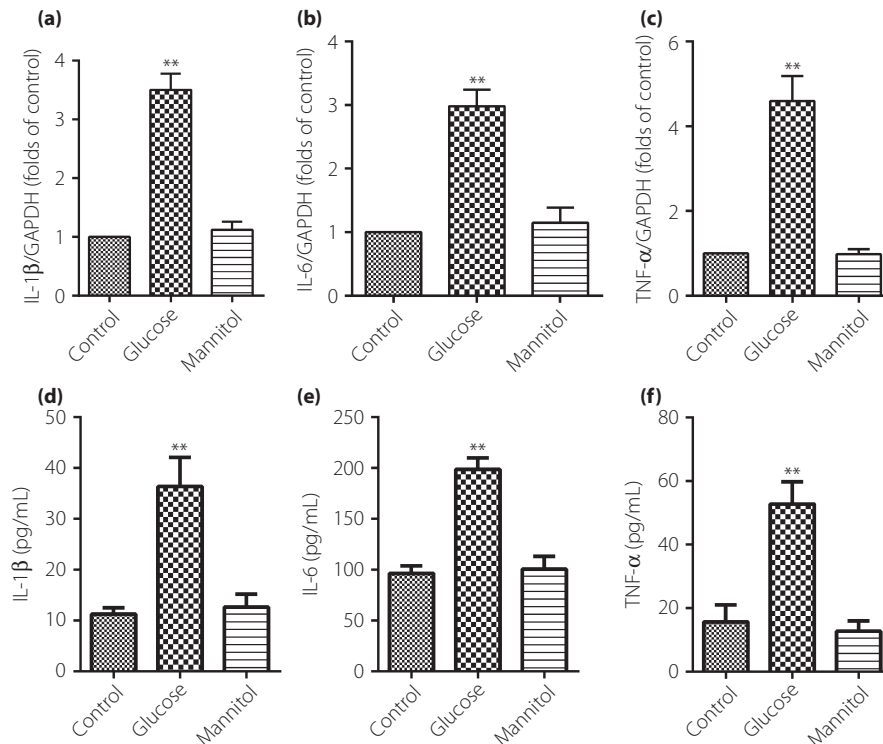


**Figure 2** | High glucose increases messenger ribonucleic acid and protein expression of interleukin (IL)-1 $\beta$ , IL-6 and tumor necrosis factor (TNF)- $\alpha$  in thoracic aorta endothelial cells. The cells were subjected to high glucose at 30 mmol/L for 12 h, then, messenger ribonucleic acid and proteins expression of IL-1 $\beta$ , IL-6 and TNF- $\alpha$  were identified by quantitative real-time polymerase chain reaction and enzyme-linked immunosorbent assay, respectively. (a–c) IL-1 $\beta$ , IL-6 and TNF- $\alpha$  messenger ribonucleic acid expression. (d–f) IL-1 $\beta$ , IL-6 and TNF- $\alpha$  proteins expression. Results were from six independent experiments for enzyme-linked immunosorbent assay and three independent experiments for quantitative real-time PCR, and expressed as mean  $\pm$  standard error of the mean. \*\* $P$  < 0.01 vs control. GAPDH, glyceraldehyde-3-phosphate dehydrogenase.

GraphPad Prism 6.0 (GraphPad Software, Inc. La Jolla, CA, USA). A  $P$ -value < .05 was considered statistically significant.

## RESULTS

### Effect of high-glucose treatment on the cell viability of TAECs

Figure 1 a showed that the cell viability of TAECs were significantly inhibited by glucose at 30 mmol/L for 12 h and showed a concentration-dependent effect; the result shown in Figure 1b indicated a time-dependent effect when subjected to glucose at 30 mmol/L. However, cells that were exposed to mannitol, an osmotic control, did not influence the growth rate of the TAECs. This suggested that high-glucose-inhibited cell viability was not a consequence of high osmolarity (Figure 1c and d).

### High glucose induces inflammatory cytokines expression in TAECs

The IL-1 $\beta$ , IL-6 and TNF- $\alpha$  mRNA were tested by real-time quantitative PCR. As shown in Figure 2a–c, IL-1 $\beta$ , IL-6 and TNF- $\alpha$  mRNA in TAECs were significantly increased after exposure to glucose at 30 mmol/L for 12 h. The results from ELISA showed that IL-1 $\beta$ , IL-6 and TNF- $\alpha$  proteins in supernate of the DMEM were significantly increased after exposure

to glucose at 30 mmol/L for 12 h compared with the control group (Figure 2d–f). However, cells exposed to mannitol did not influence the secretion of inflammatory factors of the TAECs. This suggested that high glucose increased the secretion of IL-1 $\beta$ , IL-6 and TNF- $\alpha$ , and was not a consequence of high osmolarity.

### ROS, PI3K/AKT and NF- $\kappa$ B signaling pathway involved in the inflammatory effect of high glucose in TAECs

As shown in Figure 3a, high glucose treatment was able to increase the generation of intracellular ROS in TAECs. The results from western blot showed that PI3K and phosphorylated AKT proteins expression were increased, as well as activating NF- $\kappa$ B in TAECs after the stimulation with glucose at 30 mmol/L for 12 h (Figure 3b–d). However, cells that were exposed to mannitol at 24.4 mmol/L did not affect the level of the aforementioned proteins of the TAECs. This suggested that the increased expression of PI3K, phosphorylated AKT and activating NF- $\kappa$ B as a result of high glucose was not a consequence of high osmolarity.

Further research by ELISA showed that IL-1 $\beta$ , IL-6 and TNF- $\alpha$  proteins in the supernate of DMEM were significantly

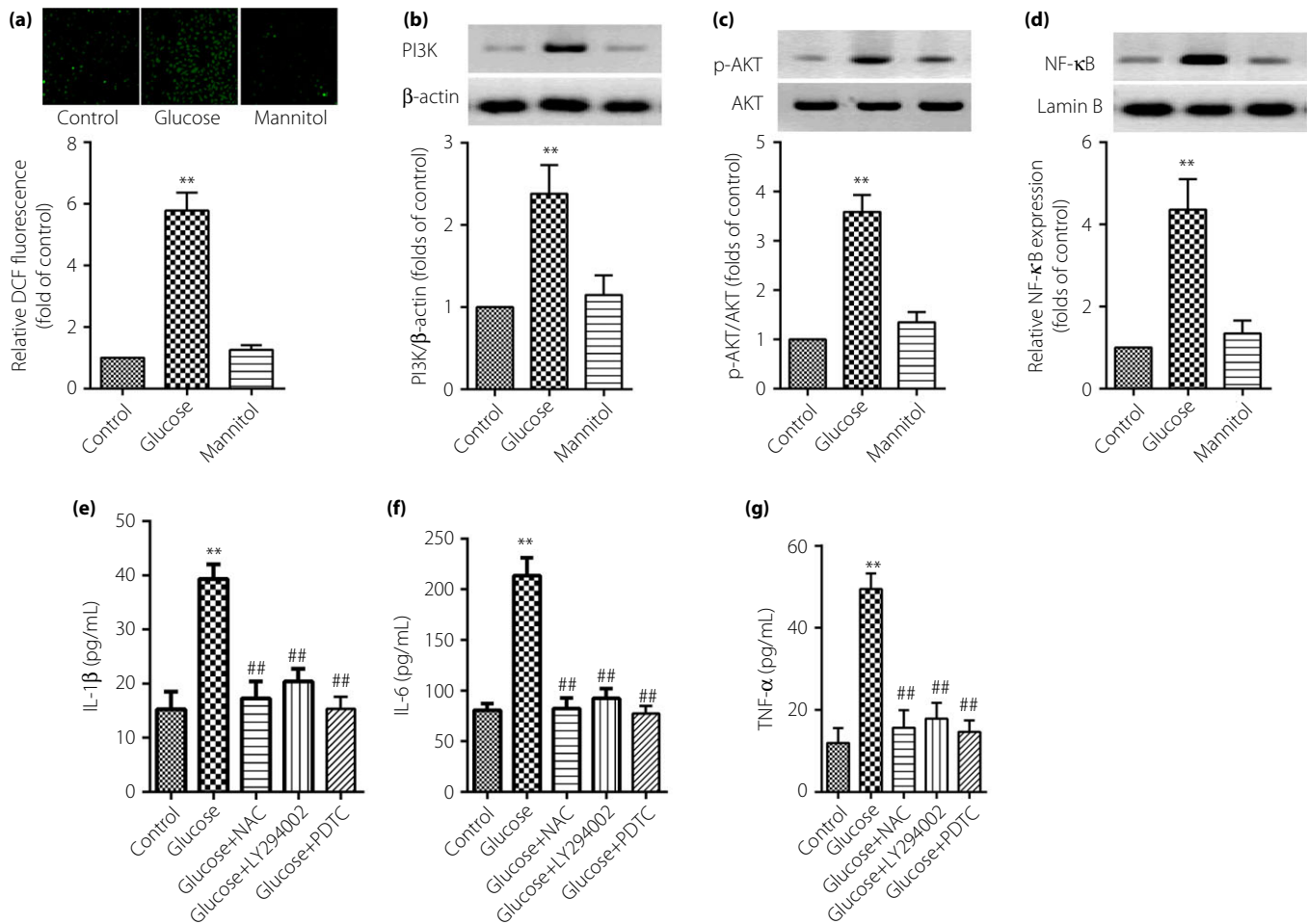


**Figure 3** | Reactive oxygen species (ROS), phosphoinositide 3-kinase (PI3K)/protein kinase B (AKT) and nuclear factor (NF)-κB signaling pathway involved in the inflammatory effect of high glucose in thoracic aorta endothelial cells. The cells were subjected to high glucose at 30 mmol/L or mannitol at 24.4 mmol/L for 12 h, then, the detection of ROS was by fluorescence microscope (magnification: ×200); (b–d) expression of PI3K, AKT and NF-κB were assayed by western blot and (e–g) proteins expression of interleukin (IL)-1β, IL-6 and tumor necrosis factor (TNF)-α were identified by enzyme-linked immunosorbent assay. Results were from six independent experiments for enzyme-linked immunosorbent assay and ROS detection, and three independent experiments for western blot. Data are expressed as mean ± standard error of the mean. \*\**P* < 0.01 vs control, ##*P* < 0.01 vs high glucose at 30 mmol/L. DCF, 2',7'-dichlorodihydrofluorescein; NAC, N-acetylcysteine.

decreased after being pretreated with LY294002 at 10 μmol/L (PI3K pathway inhibitor), PDTC (NF-κB inhibitor) at 100 μmol/L and anti-oxidant NAC at 10<sup>-2</sup> mol/L for 1 h. These results showed that the ROS–PI3K/AKT–NF-κB signaling pathway is involved in the inflammatory effect of high glucose in TAECs (Figure 3e–g).

#### Inflammatory effect induced by high glucose through the ROS–PI3K/AKT–NF-κB signaling pathway in TAECs

ROS, PI3K/AKT and NF-κB participate in the expression of inflammatory cytokines in TAECs. High glucose-induced inflammation in TAECs is possibly related to ROS–PI3K/AKT–NF-κB signaling. Pretreatment of the cells with 10<sup>-2</sup> mol/L NAC (anti-oxidant) for 1 h was able to inhibit the expression of PI3K (Figure 4a), the phosphorylation of AKT

(Figure 4b) and also decrease the activation of NF-κB (Figure 4c). These results showed that ROS are upstream of the PI3K and NF-κB signaling pathway in the inflammatory effect of high glucose in TAECs.

Further study was carried out by using 10 μmol/L LY294002 (PI3K inhibitor) to investigate the role of PI3K in the inflammatory effect of high glucose in TAECs. Data showed that LY294002 was able to inhibit the level of nuclear NF-κB expression (Figure 4e); however, the expression of ROS was not significantly decreased (Figure 4d). These data showed the inflammatory effect induced by high glucose through the ROS–PI3K–NF-κB signaling pathway in TAECs.

Finally, we explored whether the activation of NF-κB can also influence the expression of ROS and the

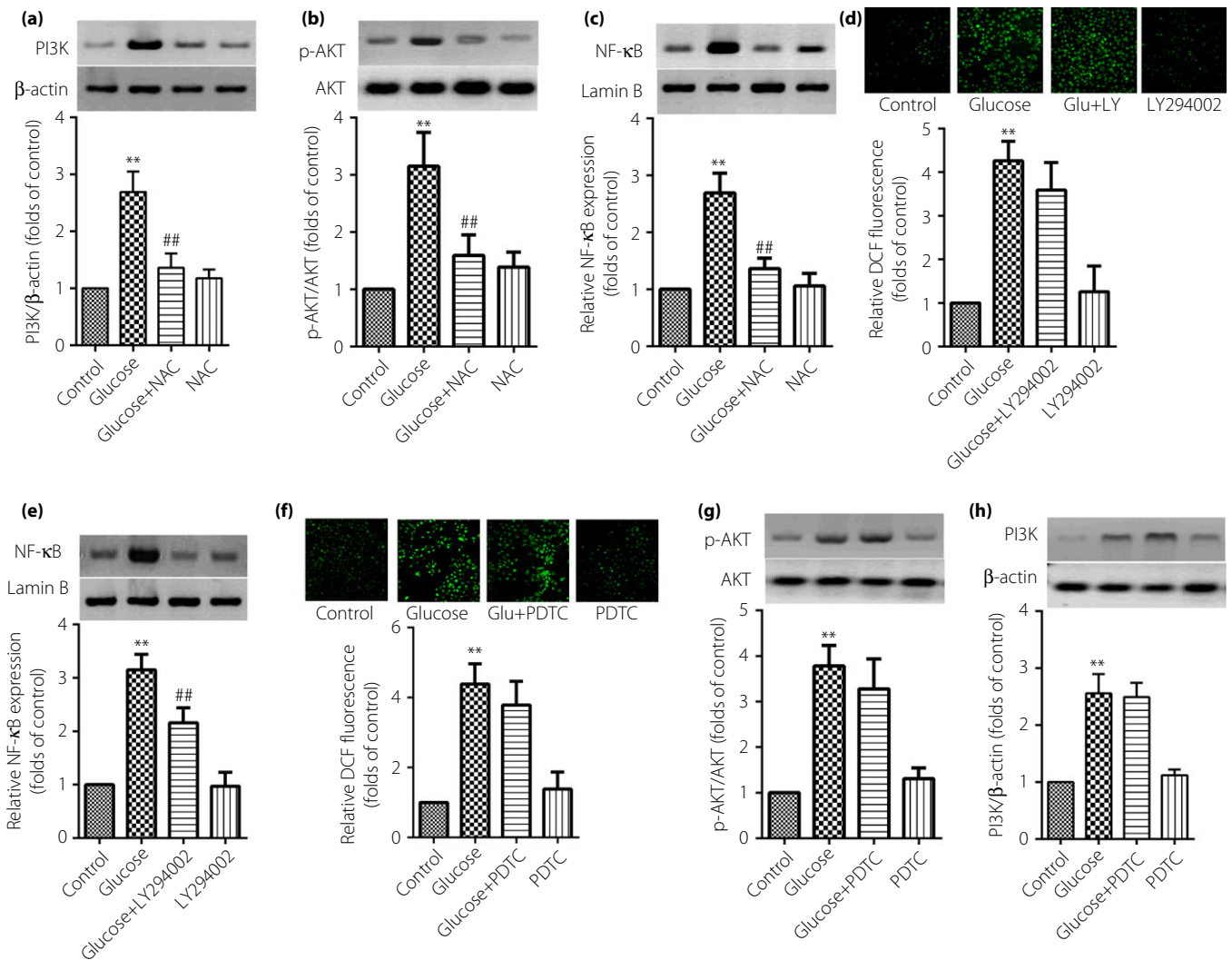


**Figure 4** | The inflammatory effect induced by high glucose through the reactive oxygen species–phosphoinositide 3-kinase (PI3K)/protein kinase B (AKT)–nuclear factor (NF)-κB signaling pathway in thoracic aorta endothelial cells. The cells were subjected to high glucose at 30 mmol/L for 12 h or in combination with the pretreatment of a related pathway inhibitor for 1 h. Then, (d,f) the detection of reactive oxygen species was by fluorescence microscope (magnification:  $\times 200$ ); (a–c,e,g,h) expression of PI3K, NF-κB or AKT were assayed by western blot. Results were from six independent experiments for reactive oxygen species detection and three independent experiments for western blot, and expressed as mean  $\pm$  standard error of the mean. \*\* $P < 0.01$  vs control, ## $P < 0.01$  vs high glucose at 30 mmol/L. NAC, N-acetylcysteine; pyrrolidine dithiocarbamate.

phosphorylation of AKT. As shown in Figure 4f and g, pretreatment with 100  $\mu\text{mol/L}$  PDTC (NF-κB inhibitor) for 1 h cannot notably affect the level of ROS and the phosphorylation of AKT. The results enhanced the aforementioned conclusion that the inflammatory effect is induced by high glucose through the ROS–PI3K–NF-κB signaling pathway in TAECs.

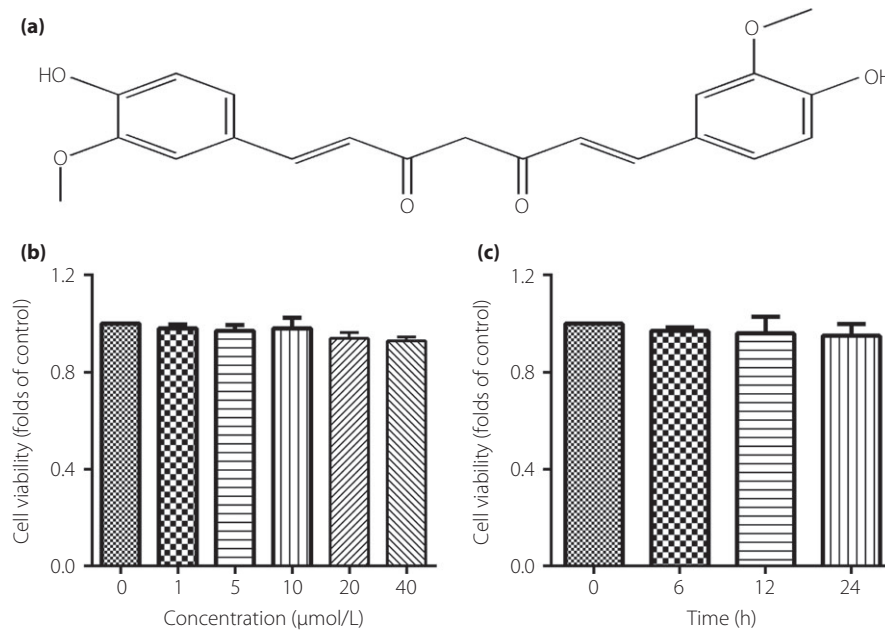
#### Effect of CUR on the cell viability TAECs

Figure 5b showed that CUR from 0–40  $\mu\text{mol/L}$  did not affect the cell viability of TAECs, when treatment with CUR at a

concentration of 10  $\mu\text{mol/L}$  for 0–24 h also showed the same effect (Figure 5c).

#### CUR attenuates high glucose-induced TAECs inflammatory damage through the ROS–PI3K/AKT–NF-κB signaling pathway

As shown in Figure 6, IL-1 $\beta$ , IL-6 and TNF- $\alpha$  proteins in TAECs were significantly decreased in the presence of CUR 10  $\mu\text{mol/L}$  for 12 h. The level of inner ROS, as well as the expression of PI3K, the phosphorylation of AKT and the activation of NF-κB were notably decreased. These results showed that the anti-inflammatory effect of CUR might be through



**Figure 5** | The effect of curcumin (CUR) on the cell viability of thoracic aorta endothelial cells. (a) The chemical structure of CUR. (b) The cells were incubated with different concentrations of CUR for 12 h. (c) The cells were incubated with concentrations of CUR at 10  $\mu\text{mol/L}$  for 0–24 h. Results were from six independent experiments and expressed as mean  $\pm$  standard error of the mean.

interfering with the ROS–PI3K/AKT–NF- $\kappa$ B signaling pathway in high-glucose-induced inflammation of TAECs.

## DISCUSSION

Hyperglycemia has been regarded as a risk factor of endothelial dysfunction, and also promotes the progression of vascular complications. High glucose could increase the risk of cell damage and dysfunction in endothelial cells. Diabetes is a greater risk for cardiovascular morbidity and mortality. Research showed that improving endothelial function and decreasing inflammation could lower cardiovascular disease risk of diabetes patients<sup>19–21</sup>. In the present study, we found that high glucose could increase the secretion of IL-1 $\beta$ , IL-6 and TNF- $\alpha$  in TAECs.

In people with diabetes, multiple organ dysfunction is mainly a result of systemic inflammatory injury of the microvasculature, especially the microvascular endothelial cells. Microvascular and microvascular endothelial cells dysfunction or injury are the initial stage of organ dysfunction. The activation of the inflammatory effect through multipathways, and oxidative damage to endothelial cells is severe in diabetes patients. ROS are both the important second messenger and the direct participant of oxidative stress. Recent research has shown that ROS plays an important role in high glucose elicited by the expression of inflammatory factors. Pro-treatment with anti-oxidant NAC at  $10^{-2}$  mol/L can significantly inhibit the expression of IL-1 $\beta$ , IL-6 and TNF- $\alpha$  proteins in TAECs.

PI3K/AKT and NF- $\kappa$ B signaling also play a pivotal role in inflammation<sup>22–27</sup>. The activation of NF- $\kappa$ B is responsible for

the expressions of many inflammatory cytokines. The present results showed that PI3K/AKT and NF- $\kappa$ B were involved in the expression of IL-1 $\beta$ , IL-6 and TNF- $\alpha$  protein induced by high glucose, as the selective PI3K/AKT LY294002 and NF- $\kappa$ B inhibitor, PDTC, significantly blocked the expression of IL-1 $\beta$ , IL-6 and TNF- $\alpha$  proteins in TAECs.

CUR – a natural compound – has attracted more and more attention for as an anti-oxidant. Results from Fazal *et al*<sup>28</sup>, showed that CUR could reduce oxidative stress in animals by scavenging ROS, protect the anti-oxidant enzymes from being denatured and reduce the oxidative stress marker lipid peroxidation. CUR also delays diabetic retinopathy through anti-oxidant and anti-inflammatory effects, and results in the inhibition of vascular endothelial growth and nuclear transcription factors<sup>29</sup>. In the present study, we showed that high glucose can increase the level of ROS and the anti-inflammatory effect of CUR mainly by blocking the expression of ROS. The PI3K/AKT signaling pathway is also a target of CUR, and Tian *et al*<sup>30,31</sup>, reported that the anti-cancer effect of CUR through mediating the PI3K/AKT/mammalian target of rapamycin signaling pathway. Our current research also showed that high glucose was able to increase the expression of PI3K and the phosphorylation of AKT in TAECs, and the anti-inflammatory effect of CUR through mediating the PI3K/AKT signaling pathway for the reason that the function of CUR is similar to the specific inhibitor of the PI3K/AKT signaling pathway. Experiments from basic research showed that CUR could attenuate acute inflammatory injury by inhibiting the TLR4/MyD88/NF- $\kappa$ B signaling pathway in experimental traumatic brain injury<sup>32</sup>,

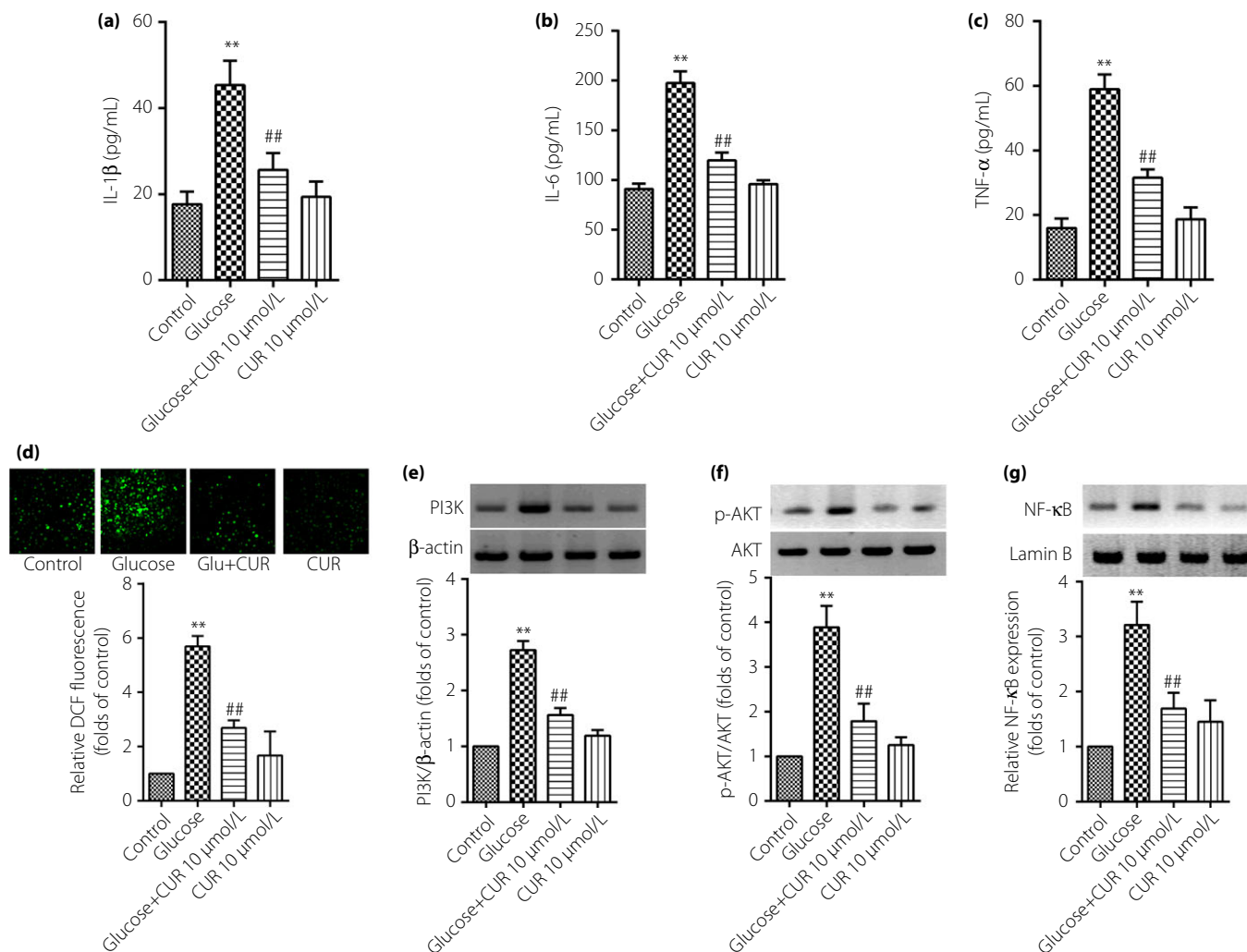


**Figure 6** | Curcumin (CUR) decreases protein expression of interleukin (IL)-1 $\beta$ , IL-6 and tumor necrosis factor (TNF)- $\alpha$  through reactive oxygen species (ROS)-phosphoinositide 3-kinase (PI3K)/protein kinase B (AKT)-nuclear factor (NF)- $\kappa$ B in thoracic aorta endothelial cells. The cells were subjected to high-glucose treatment in the absence or presence of CUR (10  $\mu$ mol/L) for 12 h. Then, protein expressions of IL-1 $\beta$ , IL-6 and TNF- $\alpha$  were identified by enzyme-linked immunosorbent assay, and the level of ROS, PI3K, AKT and NF- $\kappa$ B were detected by western blot. (a–c) IL-1 $\beta$ , IL-6 and TNF- $\alpha$  protein expression; (d–g) ROS, PI3K, AKT and NF- $\kappa$ B expression. Results were from six independent experiments for ROS detection and three independent experiments for western blot, and expressed as mean  $\pm$  standard error of the mean. \*\* $P$  < 0.01 vs control, ## $P$  < 0.01 vs high glucose at 30 mmol/L.

and decrease alveolar bone loss mainly in experimental periodontitis rats<sup>33</sup>. Another study showed that CUR could inhibit inhibitor of nuclear factor kappa-B kinase- $\alpha$ , inhibitor of nuclear factor kappa-B kinase- $\beta$  (IKK $\beta$ ) and NF- $\kappa$ B-inducing kinase, and block NF- $\kappa$ B-mediated cytokine release<sup>34</sup>. Those studies consistently showed that NF- $\kappa$ B is a target of CUR, and the present study also showed the anti-inflammatory effect of CUR through interfering with the NF- $\kappa$ B signaling pathway in high-glucose-induced inflammation.

In conclusion, the present study showed that high glucose induced the expression of IL-1 $\beta$ , IL-6 and TNF- $\alpha$  protein

through the PI3K/AKT-NF- $\kappa$ B signal pathway in TAECs. The anti-inflammatory effect of CUR might be through interfering with the PI3K/AKT-NF- $\kappa$ B signal pathway in TAECs. These provide new evidence for the potential inflammatory effect of high glucose and a strategy of dealing with high-glucose-induced inflammation.

#### ACKNOWLEDGMENTS

We are grateful for the financial support of the First People's Hospital of Shangqiu. The authors thank Prof. Cao Hui for helpful discussions.



**DISCLOSURE**

The authors declare no conflict of interest.

**REFERENCES**

- Li ZY, Zheng Y, Chen Y, *et al.* Brazilin ameliorates diabetic nephropathy and inflammation in db/db mice. *Inflammation* 2017; 40: 1365–1374.
- Zhou XY, Zhang F, Hu XT, *et al.* Depression can be prevented by astaxanthin through inhibition of hippocampal inflammation in diabetic mice. *Brain Res* 2017; 1657: 262–268.
- Babu PV, Si H, Fu Z, *et al.* Genistein prevents hyperglycemia-induced monocyte adhesion to human aortic endothelial cells through preservation of the cAMP signaling pathway and ameliorates vascular inflammation in obese diabetic mice. *J Nutr* 2012; 142: 724–730.
- Wang Y, Fan L, Meng X, *et al.* Transplantation of IL-10-transfected endothelial progenitor cells improves retinal vascular repair via suppressing inflammation in diabetic rats. *Graefes Arch Clin Exp Ophthalmol* 2016; 254: 1957–1965.
- Zhang Z, Li Y, Li Y. Grape seed proanthocyanidin extracts prevent hyperglycemia-induced monocyte adhesion to aortic endothelial cells and ameliorates vascular inflammation in high-carbohydrate/high-fat diet and streptozotocin-induced diabetic rats. *Int J Food Sci Nutr* 2015; 67: 524–534.
- Kanashiro A, Sonogo F, Ferreira RG, *et al.* Therapeutic potential and limitations of cholinergic anti-inflammatory pathway in sepsis. *Pharmacol Res* 2017; 117: 1–8.
- Doerschug KC, Delsing AS, Schmidt GA, *et al.* Impairments in microvascular reactivity are related to organ failure in human sepsis. *Am J Physiol Heart Circ Physiol* 2007; 293: H1065–H1071.
- Georgiopoulos G, Lambrinouadaki I, Athanasouli F, *et al.* Prolactin as a predictor of endothelial dysfunction and arterial stiffness progression in menopause. *J Hum Hypertens* 2017; 31: 520–524.
- Baghdasaryan A, Claudel T, Kusters A, *et al.* Curcumin improves sclerosing cholangitis in Mdr2<sup>-/-</sup> mice by inhibition of cholangiocyte inflammatory response and portal myofibroblast proliferation. *Gut* 2010; 59: 521–530.
- Bisht S, Khan MA, Bekhit M, *et al.* A polymeric nanoparticle formulation of curcumin (NanoCurc) ameliorates CCl<sub>4</sub>-induced hepatic injury and fibrosis through reduction of pro-inflammatory cytokines and stellate cell activation. *Lab Invest* 2011; 91: 1383–1395.
- Fu Y, Gao R, Cao Y, *et al.* Curcumin attenuates inflammatory responses by suppressing TLR4-mediated NF-kappaB signaling pathway in lipopolysaccharide-induced mastitis in mice. *Int Immunopharmacol* 2014; 20: 54–58.
- Choudhury AK, Raja S, Mahapatra S, *et al.* Synthesis and evaluation of the anti-oxidant capacity of curcumin Glucuronides, the major curcumin metabolites. *Antioxidants* 2015; 4: 750–767.
- Mandal MN, Patlolla JM, Zheng L, *et al.* Curcumin protects retinal cells from light-and oxidant stress-induced cell death. *Free Radic Biol Med* 2009; 46: 672–679.
- Xie M, Fan D, Zhao Z, *et al.* Nano-curcumin prepared via supercritical: improved anti-bacterial, anti-oxidant and anti-cancer efficacy. *Int J Pharm* 2015; 496: 732–740.
- Das L, Vinayak M. Anti-carcinogenic action of curcumin by activation of antioxidant defence system and inhibition of NF-kappaB signalling in lymphoma-bearing mice. *Biosci Rep* 2012; 32: 161–170.
- Heng MC. Curcumin targeted signaling pathways: basis for anti-photoaging and anti-carcinogenic therapy. *Int J Dermatol* 2010; 49: 608–622.
- Samuels TL, Pearson AC, Wells CW, *et al.* Curcumin and anthocyanin inhibit pepsin-mediated cell damage and carcinogenic changes in airway epithelial cells. *Ann Otol Rhinol Laryngol* 2013; 122: 632–641.
- Kevil CG, Bullard DC. In vitro culture and characterization of gene targeted mouse endothelium. *Acta Physiol Scand* 2001; 173: 151–157.
- Ishibashi Y, Matsui T, Matsumoto T, *et al.* Ranirestat has a stronger inhibitory activity on aldose reductase and suppresses inflammatory reactions in high glucose-exposed endothelial cells. *Diab Vasc Dis Res* 2016; 13: 312–315.
- He X, Ou C, Xiao Y, *et al.* Atorvastatin inhibits the inflammatory injury of human umbilical vein endothelial cells induced by high glucose by regulating the expression of MALAT1. *Diabetes Metab Res Rev* 2016; 32: 24–25.
- Zhao Q, Gao C, Cui Z. Ginkgolide A reduces inflammatory response in high-glucose-stimulated human umbilical vein endothelial cells through STAT3-mediated pathway. *Int Immunopharmacol* 2015; 25: 242–248.
- O'Sullivan AW, Wang JH, Redmond HP. NF-kappaB and p38 MAPK inhibition improve survival in endotoxin shock and in a cecal ligation and puncture model of sepsis in combination with antibiotic therapy. *J Surg Res* 2009; 152: 46–53.
- Ronco MT, Manarin R, Frances D, *et al.* Benzimidazole treatment attenuates liver NF-kappaB activity and MAPK in a cecal ligation and puncture model of sepsis. *Mol Immunol* 2011; 48: 867–873.
- Song GY, Chung CS, Chaudry IH, *et al.* Immune suppression in polymicrobial sepsis: differential regulation of Th1 and Th2 responses by p38 MAPK. *J Surg Res* 2000; 91: 141–146.
- Song GY, Chung CS, Jarrar D, *et al.* Evolution of an immune suppressive macrophage phenotype as a product of P38 MAPK activation in polymicrobial sepsis. *Shock* 2001; 15: 42–48.
- Song GY, Chung CS, Jarrar D, *et al.* Mechanism of immune dysfunction in sepsis: inducible nitric oxide-mediated alterations in p38 MAPK activation. *J Trauma* 2002; 53: 276–282; discussion 282–273.

27. Sun Y, Li YH, Wu XX, *et al.* Ethanol extract from *Artemisia vestita*, a traditional Tibetan medicine, exerts anti-sepsis action through down-regulating the MAPK and NF-kappaB pathways. *Int J Mol Med* 2006; 17: 957–962.
28. Fazal Y, Fatima SN, Shahid SM, *et al.* Effects of curcumin on angiotensin-converting enzyme gene expression, oxidative stress and anti-oxidant status in thioacetamide-induced hepatotoxicity. *J Renin Angiotensin Aldosterone Syst (JRAAS)* 2015; 16: 1046–1051.
29. Aldebasi YH, Aly SM, Rahmani AH. Therapeutic implications of curcumin in the prevention of diabetic retinopathy via modulation of anti-oxidant activity and genetic pathways. *Int J Physiol Pathophysiol Pharmacol* 2013; 5: 194–202.
30. Tian B, Zhao Y, Liang T, *et al.* Curcumin inhibits urothelial tumor development by suppressing IGF2 and IGF2-mediated PI3K/AKT/mTOR signaling pathway. *J Drug Target* 2017; 25: 626–636.
31. Cianciulli A, Calvello R, Porro C, *et al.* PI3k/Akt signalling pathway plays a crucial role in the anti-inflammatory effects of curcumin in LPS-activated microglia. *Int Immunopharmacol* 2016; 36: 282–290.
32. Zhu HT, Bian C, Yuan JC, *et al.* Curcumin attenuates acute inflammatory injury by inhibiting the TLR4/MyD88/NF-kappaB signaling pathway in experimental traumatic brain injury. *J Neuroinflammation* 2014; 11: 59.
33. Zhou T, Chen D, Li Q, *et al.* Curcumin inhibits inflammatory response and bone loss during experimental periodontitis in rats. *Acta Odontol Scand* 2013; 71: 349–356.
34. Wessler S, Muenzner P, Meyer TF, *et al.* The anti-inflammatory compound curcumin inhibits *Neisseria gonorrhoeae*-induced NF-kappaB signaling, release of pro-inflammatory cytokines/chemokines and attenuates adhesion in late infection. *Biol Chem* 2005; 386: 481–490.

## SUPPORTING INFORMATION

Additional Supporting Information may be found in the online version of this article:

**Figure S1** | Characterization of the primary cultured thoracic aorta endothelial cells derived from the thoracic aortae of male Sprague–Dawley rats.